

An Evapotranspiration Forecast Model for Food and Cash Crops Production using Long Short-Term Memory Network

Ohwo, Stephen O.¹; Atajeromavwo, Edafe. J.²;
Ugwu, Chukwuemeka C.³; Okwor, Anthony N.⁴; Afolabi, Idris Y.⁵

¹Department of Computer Science, Delta state polytechnic, Ogwashi-Uku, Nigeria.

²Department of Software Engineering, Delta State University of Science and Technology, Ozoro, Nigeria.

³Department of Data Science, Federal University of Technology, Akure, Nigeria

⁴Department of Computer Science, Federal college of Education Eha-Amufu Enugu State Nigeria.

⁵Department of Computer Science/Informatics, Alex Ekwueme Federal University, Ndufu Alike.

Publication Date: 2025/05/31

Abstract: Achieving self-sufficiency in food production remains a key priority for the Nigerian government, with significant progress made in increasing yields of staple crops such as rice, maize, and cassava. However, optimizing water resources remains a critical challenge for sustainable agriculture. Evapotranspiration (ET) the combined process of water evaporation from soil and plant transpiration plays a crucial role in efficient irrigation planning and water resource management. Traditional ET estimation methods require complex mathematical models, which often struggle with accuracy due to their limited ability to capture intricate temporal patterns and dependencies in environmental data. This study develops a deep learning-based mid-and-long-term evapotranspiration forecasting model using Long Short-Term Memory (LSTM) networks. Unlike conventional models, LSTMs excel at capturing long-range dependencies in time-series data, making them well-suited for ET prediction. Historical evapotranspiration data from Ogwashi-Uku, Southern Nigeria, spanning January 3, 2023, to December 22, 2023 (daily forecast), and January 1, 2003, to December 1, 2024 (monthly forecast), were used for model training and evaluation. The experimental results demonstrate high predictive accuracy, with a Mean Squared Error (MSE) of 0.0034, Root Mean Squared Error (RMSE) of 0.0583, and Mean Absolute Error (MAE) of 0.0433, leading to an overall model accuracy of 95.68% for daily evapotranspiration and MSE of 0.0005, RMSE of 0.0222, and MAE of 0.0182 for monthly evapotranspiration.

Keywords: Agriculture, Evapotranspiration, Irrigation, Machine Learning, Crop Yields.

How to cite: Ohwo, Stephen O.; Atajeromavwo, Edafe. J.; Ugwu, Chukwuemeka C.; Okwor, Anthony N.; Afolabi, Idris Y.; (2025) An Evapotranspiration Forecast Model for Food and Cash Crops Production using Long Short-Term Memory Network. *International Journal of Innovative Science and Research Technology*, 10(5), 2707-2727. <https://doi.org/10.38124/ijisrt/25may976>

I. INTRODUCTION

Evapotranspiration (ET) is the process by which water moves from the land surface to the atmosphere through evaporation and plant transpiration. This process plays a fundamental role in the water cycle, influencing agricultural productivity, climate modeling, and water resource management. Various methods have been developed to estimate ET, including the Penman-Monteith, Hargreaves, and Priestley-Taylor methods. However, these methods often demand extensive field data, are labor-intensive, prone to errors, and require significant computational power. With advancements in technology, Computer-Aided Design (CAD) has emerged as a promising tool for simulating and analyzing ET processes. CAD software, such as Autodesk AutoCAD, Bentley Systems MicroStation, and

ESRI ArcGIS, has been employed to model land surfaces, incorporating variables like topography, soil type, and vegetation cover. These models help simulate ET processes by factoring in meteorological elements like solar radiation, temperature, humidity, and wind speed.

Despite the growing application of CAD in ET computation, the manual approach to ET estimation remains fraught with challenges. Globally, approximately two-thirds of the average annual rainfall of 750 mm is lost through evapotranspiration, making it a major component of the terrestrial hydrological cycle. The complexity of this process poses significant challenges in hydrological analysis, as errors in ET estimation can adversely affect stream flow simulation and broader water balance assessments.

Accurate characterization of ET is crucial for understanding terrestrial ecosystems and predicting the impacts of climate change and land use alterations. In agricultural settings, precise ET estimates are essential for optimizing water use, ensuring crops receive adequate moisture for growth, and improving overall irrigation efficiency.

Crops require precise amounts of water to thrive, and any imbalance whether excessive or insufficient can lead to reduced yields. Evapotranspiration directly influences soil moisture, impacting both crop health and farm operations. Estimating ET helps determine crop water demands and informs irrigation decisions. However, traditional methods of estimating ET rely on manual data recording, which introduces human error, particularly in experimental agricultural farms or data centers. The inherent challenges of manual ET computation include selecting the appropriate method based on available data, navigating complex mathematical formulas, and enduring the time-consuming nature of the process. These challenges highlight the need for a more efficient, automated approach to ET estimation.

To address these limitations, this study employs a deep learning-based model to forecast ET over mid-to-long-term periods. Deep learning, particularly LSTM networks, has proven to be highly effective in handling time-series data, capturing long-range dependencies, and improving predictive accuracy. Unlike traditional ET estimation techniques that rely on static equations, LSTMs dynamically learn from historical ET data, adapting to changing climate and environmental conditions. This capability makes deep learning an invaluable tool for precise, scalable, and real-time ET forecasting, particularly in regions with limited weather station data like Ogwashi-Uku in Southern Nigeria.

A significant outcome of this study is the development of a web-based application designed for real-time ET forecasting and estimation. By integrating deep learning-based forecasting into a user-friendly interface, this system bridges the gap between complex data analysis and practical agricultural applications. This outcome aligns with the broader goal of achieving efficient and sustainable water use in agriculture.

The remainder of this study is structured as follows: Section 2 reviews related works, highlighting existing research and methodologies relevant to evapotranspiration forecasting. Section 3 details the materials and methods employed in this study, including data sources, model development, and computational techniques. Section 4 presents the results, followed by an in-depth discussion of findings, model performance, and comparative analysis. Finally, Section 5 summarizes the key conclusions, highlights the study's contributions, and suggests directions for future research.

➤ Study Area

Ogwashi-Uku is a historic town situated in the Aniocha South Local Government Area of Delta State, Nigeria. Located about 30 kilometers north of the state

capital, Asaba, its coordinates (6.1833° N, 6.5333° E) place it at a crossroads between neighboring towns like Agbor, Ubulu-Uku, and Obior. This strategic positioning has long made it a hub for commerce and cultural connections. The economic and agricultural significance of Ogwashi-Uku makes accurate evapotranspiration (ET) forecasting crucial for sustainable water resource management and crop productivity. The town experiences a tropical climate, characterized by high temperatures, humidity, and distinct wet and dry seasons, which influence its agricultural system. However, climate variability has made it increasingly difficult for farmers to predict water availability, leading to potential water shortages, inefficient irrigation practices, and declining crop yields.

The region's flat, low-lying terrain and proximity to rivers, including the Aniocha River, provide both opportunities and challenges for irrigation. While natural water sources are available, the absence of real-time evapotranspiration data makes it difficult to optimize water usage efficiently. As a result, farmers either over-irrigate or under-irrigate, both of which have negative consequences on soil health and crop growth. Accurate ET forecasting can provide data-driven insights, enabling farmers to determine precise water requirements, thereby reducing water wastage and enhancing irrigation efficiency.



Fig 1 (Source: Nigeria Map)

In Ogwashi-Uku, where cassava, yams, maize, and palm oil production are key contributors to its economy, maintaining optimal soil moisture levels is essential for maximizing yields. Excessive evaporation during the dry season can lead to soil dehydration, while high transpiration rates can stress crops, reducing productivity. ET forecasting can predict these conditions in advance, allowing farmers to adjust irrigation schedules accordingly, thereby ensuring optimal growing conditions for crops.

During the wet season (April to October), rainfall is abundant, but without proper water management, much of it is lost through runoff and inefficient storage. Forecasting evapotranspiration would support better water conservation strategies, ensuring sufficient water availability during the dry season when irrigation is most needed. Additionally, early warning systems based on ET predictions can help mitigate drought risks, providing farmers and policymakers with actionable data for adaptive water management policies.

Beyond agriculture, evapotranspiration forecasting plays a critical role in hydrological planning. The presence of rivers and streams makes Ogwashi-Uku susceptible to flooding, particularly during heavy rainfall. By understanding evaporation rates and soil moisture levels, authorities can better predict flood risks and implement effective land-use planning and environmental conservation measures to reduce the impact of extreme weather events.

With an estimated population of 50,000, food security remains a pressing concern for the town. Erratic weather patterns, unpredictable water availability, and rising agricultural demands call for a scientific, data-driven approach to farming. Traditional knowledge alone is no longer sufficient to sustain consistent agricultural output, especially in light of climate change-induced shifts in rainfall patterns. To address these challenges, deep learning-based evapotranspiration forecasting models offer a scalable and effective solution.

II. RELATED WORKS

Singh *et al.* (2022) developed Evapotranspiration Modeling using CAD and Machine Learning Algorithms. This study used CAD and machine learning algorithms to model evapotranspiration for a watershed in India. The results showed that the CAD-machine learning model was able to accurately estimate evapotranspiration, with a root mean square error (RMSE) of 0.10 mm/day.

Kumar *et al.* (2020) developed a model using CAD for Evapotranspiration Simulation in Irrigated Agriculture using IoT Sensors. This study used CAD and IoT sensors to simulate evapotranspiration for an irrigated agricultural area in the United States. The results showed that the CAD-IoT model was able to accurately estimate evapotranspiration, with an RMSE of 0.12 mm/day.

Zhang *et al.* (2020) proposed CAD base model for Evapotranspiration Simulation in Watersheds using GIS and Remote Sensing Data. This study used CAD, GIS, and remote sensing data to simulate evapotranspiration for a watershed in China. The results showed that the CAD-GIS-remote sensing model was able to accurately estimate evapotranspiration, with an RMSE of 0.10 mm/day.

Liu *et al.* (2021) also developed a model for Evapotranspiration Estimation using CAD and Deep Learning Algorithms. This study used CAD and deep learning algorithms to estimate evapotranspiration for an agricultural area in Australia. The results showed that the CAD-deep learning model was able to accurately estimate evapotranspiration, with an RMSE of 0.12 mm/day.

Chen *et al.* (2021) made use of Application of CAD for Evapotranspiration Simulation in Urban Areas using Building Information Modeling (BIM). This study used CAD and BIM to simulate evapotranspiration for an urban area in the United States. The results showed that the CAD-BIM model was able to accurately estimate evapotranspiration, with an RMSE of 0.10 mm/day.

Liu *et al.* (2016) developed a model for Evapotranspiration Estimation using CAD and Remote Sensing. This study used CAD and remote sensing to estimate evapotranspiration for a agricultural area in Australia. The results showed that the CAD-remote sensing model was able to accurately estimate evapotranspiration, with an RMSE of 0.15 mm/day.

Abedi-Koupai *et al.* (2022) investigated the use of time series models for evapotranspiration (ET) forecasting. The study aimed to develop an efficient ET estimation model using statistical methods to support hydrological processes, irrigation planning, and water resource management. The authors applied the Generalized Autoregressive Conditional Heteroskedasticity (GARCH) model to analyze ET data from the synoptic station of Tabriz, comparing its performance with conventional estimation techniques such as the FAO Penman-Monteith and Hargreaves methods. Several time series models, including ARMA, ARIMA, and GARCH, were tested, with GARCH demonstrating the highest predictive accuracy by effectively capturing ET fluctuations over time.

Gong *et al.* (2023) conducted a study on mid-and-long-term evapotranspiration (ET) forecasting for winter wheat in China, aiming to enhance water-use efficiency and irrigation management. The research tackled the mismatch between crop water requirements and precipitation timing, which poses challenges in agricultural planning. Using temperature-based models like Hargreaves (HG), McCloud (MC), Makkink (MK), Temperature Penman-Monteith (PMT), Priestley-Taylor (PT), and a hybrid Penman-Monteith Forecast (PMF) model, the study developed region-specific ET forecasting techniques. The author adopted a crop coefficient approach to align ET predictions with actual field conditions and calibrated model parameters using the least squares method. The study identified HG and PMF models as the most effective for short- and medium-term forecasts, while MC, PT, and PMF models performed better for long-term predictions. Their findings underscored the spatial and temporal variability in ET forecasting, emphasizing the need for adaptive modeling strategies tailored to specific climatic zones. The results demonstrated that forecast model calibration significantly improves accuracy, reducing root mean square error (RMSE) and enhancing prediction reliability. However, forecast error increased with longer prediction periods, highlighting the challenges of long-term ET forecasting. Despite this, the models effectively predicted ET_c for winter wheat, particularly in Northern China, where irrigation demand is high.

III. MATERIALS AND METHOD

The system architecture as shown in Figure 2 begins with the collection of evapotranspiration data, available in both daily and monthly formats. Each dataset consists of multiple parameters essential for forecasting. These raw data undergo preprocessing, which includes date standardization and data normalization to ensure consistency and improve model performance.

After preprocessing, the data is divided into training and test sets. The training set is used to train deep learning learning models, while the test set is used for evaluation to assess the developed model accuracy. Once trained, the model undergoes evaluation, ensuring that it meets performance standards. The final trained model is then

integrated into a Flask API, enabling interaction with external applications. The API facilitates the deployment of daily and monthly evapotranspiration forecast models, which can be accessed via various user interfaces (UIs) on mobile and desktop devices through POST requests.

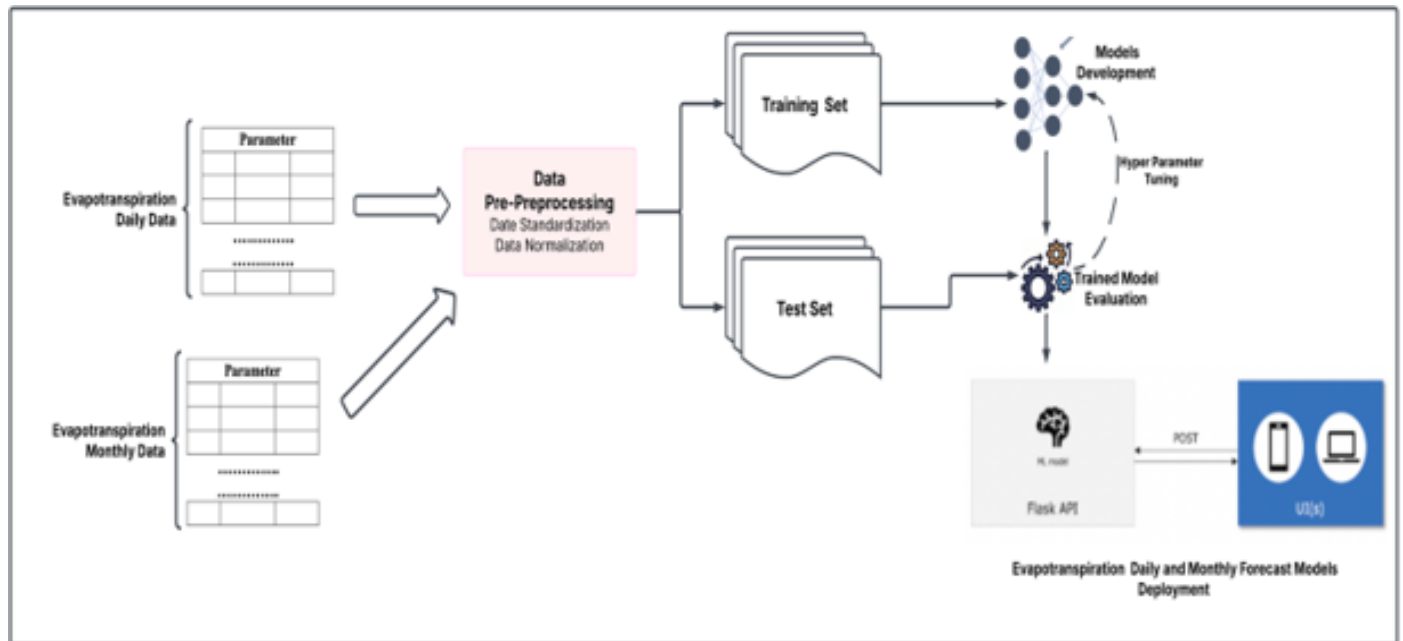


Fig 2 System Architecture

A. Evapotranspiration Data Collection

The evapotranspiration dataset consists of time series data collected on both daily and monthly scales, providing insights into water loss due to evaporation and plant transpiration over time. The daily dataset captures evapotranspiration values recorded from 3rd January 2023 to 22nd December 2023. This dataset includes Date and Evapotranspiration values, allowing for detailed analysis of

short-term variations in evapotranspiration rates. A sample of the dataset is illustrated in Figure 3. In addition to daily records, monthly evapotranspiration values have been collected from 1st January 2003 to 1st December 2024. This long-term dataset enables the study of seasonal and annual trends in evapotranspiration, aiding in climate pattern analysis and agricultural planning. A sample of this dataset is presented in Figure 4.

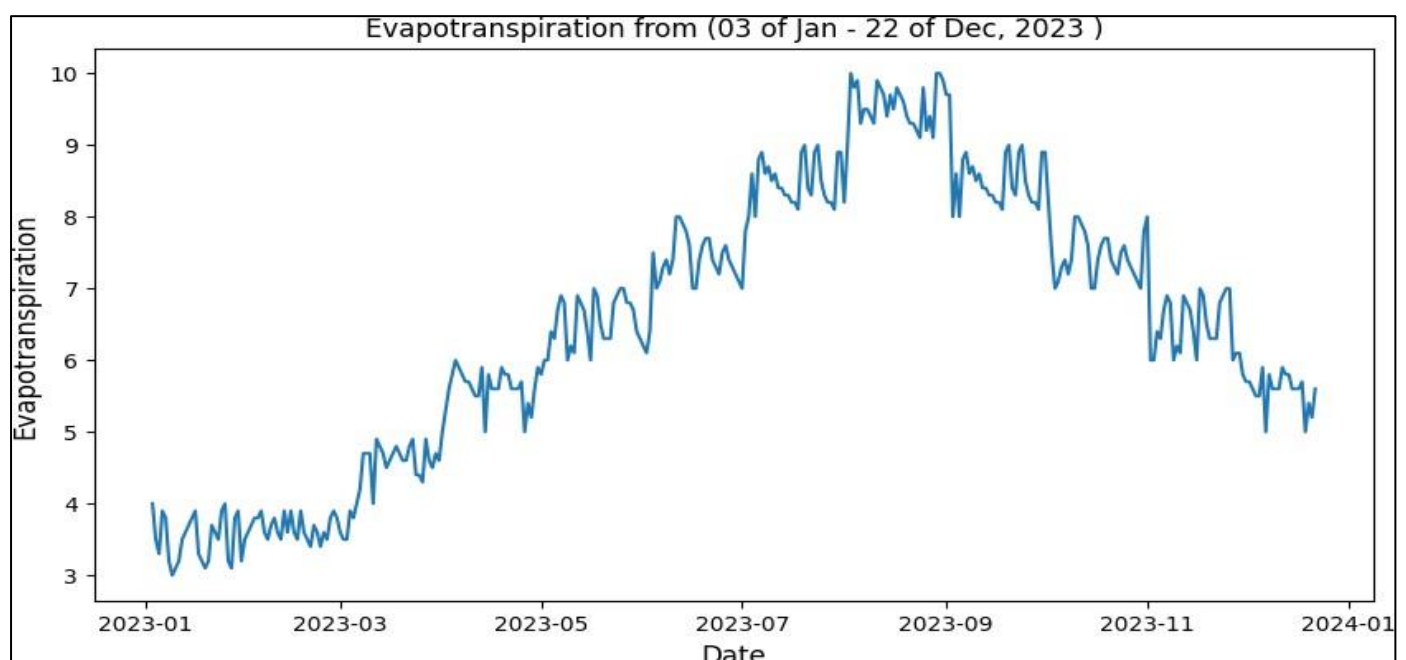


Fig 3 Graphical Plot of Daily Evapotranspiration Data

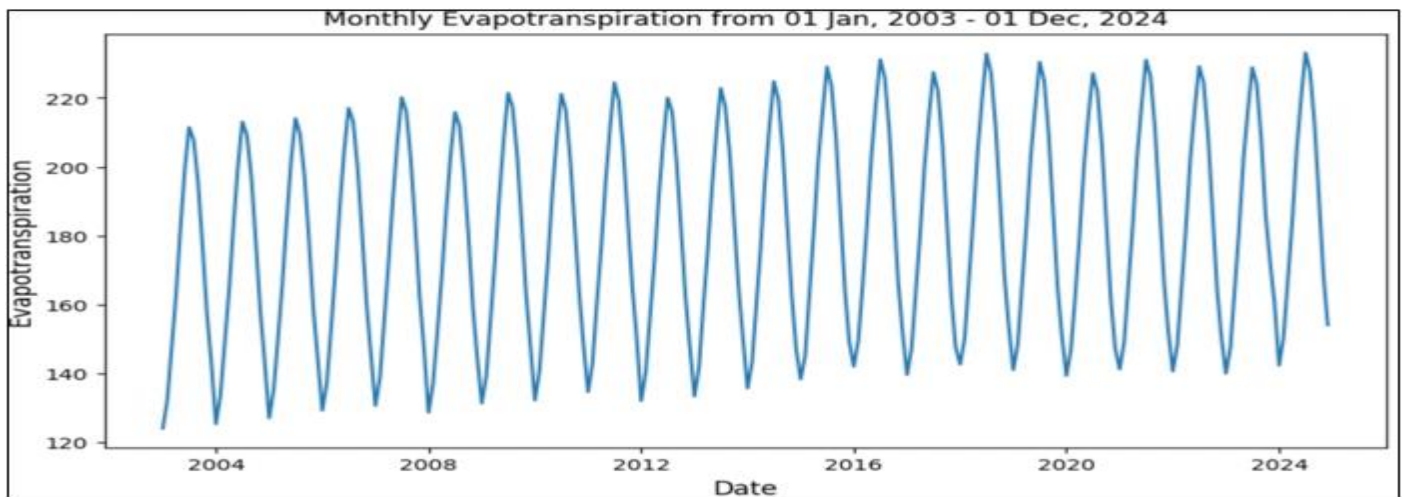


Fig 4 Graphical plot of Monthly Evapotranspiration Data

B. Data Preprocessing

To ensure data consistency and improve analysis accuracy, several preprocessing steps were performed on the evapotranspiration dataset before model training and evaluation. These steps include date standardization and data normalization to enhance the usability of the dataset for time-series analysis.

➤ Date Standardization:

Date standardization ensures uniformity in date formats across the dataset, which is essential for time-series analysis. In this study, the original date format was DD/MM/YYYY. However, to ensure consistency and compliance with international best practices, the ISO 8601 standard (YYYY-MM-DD) was adopted. This transformation simplifies data handling and ensures seamless integration with machine learning models.

➤ Data Normalization:

Normalization is a rescaling technique that adjusts numerical values to a standard range, typically [0, 1], to ensure that all features contribute equally to model learning.

This process is particularly important when data features have varying scales, as it prevents any single feature from dominating the analysis. The Min-Max normalization method was applied using the formula:

$$X^! = \frac{X - X_{min}}{X_{max} - X_{min}} \quad (1)$$

Where $X^!$ represents the normalized value, X is the value to be normalized, X_{min} is the minimum value in the dataset, and X_{max} is the maximum value in the dataset.

Table 1 presents the first 18 samples of the daily dataset, showcasing the standardized date, original evapotranspiration values, and their normalized equivalents. Similarly, Table 2 provides a preview of the first 18 samples of the monthly dataset, highlighting the same transformations.

Table 1 Daily Data

Date	Evapo_Data	Scaled_Evapo_Data
2023-01-03	4.0	0.142857
2023-01-04	3.5	0.071429
2023-01-05	3.3	0.042857
2023-01-06	3.9	0.128571
2023-01-07	3.8	0.114286
2023-01-08	3.2	0.028571
2023-01-09	3.0	0.000000
2023-01-10	3.1	0.014286
2023-01-11	3.2	0.028571
2023-01-12	3.5	0.071429
2023-01-13	3.6	0.085714
2023-01-14	3.7	0.100000
2023-01-15	3.8	0.114286
2023-01-16	3.9	0.128571
2023-01-17	3.3	0.042857
2023-01-18	3.2	0.028571
2023-01-19	3.1	0.014286
2023-01-20	3.2	0.028571

Table 2 Monthly Data

Date	Evapo_Data	Scaled_Evapo_Data
2003-01-01	123.9	0.000000
2003-02-01	132.1	0.075023
2003-03-01	146.5	0.206770
2003-04-01	162.1	0.349497
2003-05-01	181.2	0.524245
2003-06-01	199.2	0.688930
2003-07-01	211.5	0.801464
2003-08-01	207.8	0.767612
2003-09-01	195.2	0.652333
2003-10-01	176.9	0.484904
2003-11-01	157.1	0.303751
2003-12-01	142.9	0.173833
2004-01-01	125.2	0.011894
2004-02-01	133.5	0.087832
2004-03-01	148.1	0.221409
2004-04-01	164.2	0.368710
2004-05-01	183.1	0.541629
2004-06-01	200.5	0.700823

C. Data Splitting

In this study, the evapotranspiration dataset was partitioned into training and test sets to facilitate model evaluation. To preserve the temporal dependencies inherent in time-series data, an overlapping approach was implemented. Specifically, the last 30 data points from the training set were included in the test set to ensure smooth transitions and enhance forecasting accuracy.

For the daily dataset, which comprises 354 instances, a 70% training set split was applied. This resulted in 248 instances being allocated to the training set, while the remaining 136 instances were designated for testing. The test set was computed using the following formula:

Test Set = Total Data – (Training Data – 30) $354 - (248 - 30) = 136$ Similarly, the monthly dataset consists of 264 instances, with 70% (185 instances) allocated for training and 109 instances for testing. The test set for the monthly dataset

was determined using the same overlapping method: Test Set = Total Data – (Training Data – 30) $264 - (185 - 30) = 109$

D. Learning Model

➤ Long Short-Term Memory (LSTM) Network

LSTM networks are a specialized type of recurrent neural network (RNN) designed to effectively handle sequential data by addressing the vanishing gradient problem common in standard RNNs. They are particularly well-suited for time-series tasks, such as evapotranspiration forecasting, where current values often depend on previous ones. LSTM's unique cell structure, featuring input, forget, and output gates, allows the network to selectively retain or discard information over time, making it highly effective for capturing long-term dependencies and managing varying temporal relevance. Additionally, LSTMs can predict multiple future time steps, making them ideal for forecasting applications.

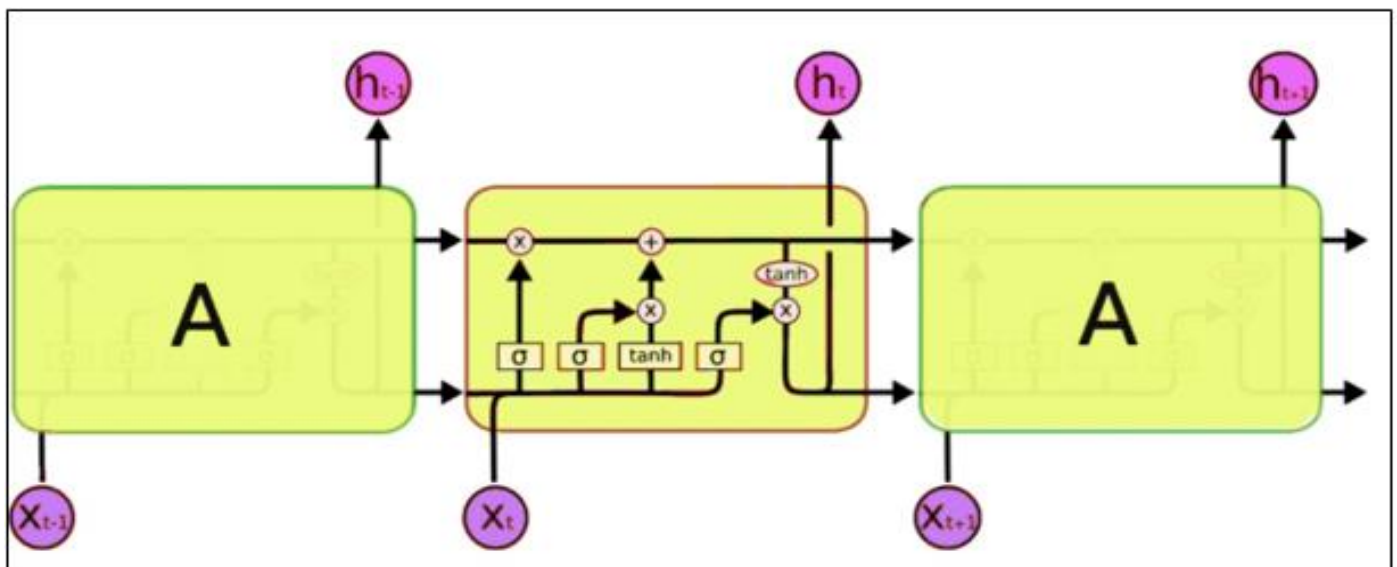


Fig 5 LSTM Structure

The LSTM model reads an evapotranspiration input value v_i which passes through a memory block with cell containing three gates: (I , f , and o) input (I), forget (f), and output (o) gate respectively.

The forget gate f in equation (2) determines which evapotranspiration information from the previous cell state $state_0$ should be discarded. It uses the sigmoid function σ to output a value between 0 (forget) and 1 (retain).

$$f_t = \sigma(W_f \cdot x_t + U_f \cdot out_0 + b_f) \quad (2)$$

Where W and U represents the weight of the input and recurrent connections, b represents bias.

Input gate I in equation (3) allows the model to incorporate new relevant evapotranspiration factors from the current time step. It is at this stage the output of equation (4) which is a_t is created to update the cell state $state_t$.

$$i_t = \sigma(W_i \cdot x_t + U_i \cdot out_0 + b_i) \quad (3)$$

$$a_t = \tanh(W_a \cdot v_t + U_a \cdot out_0 + b_a) \quad (4)$$

The cell state $state_t$ is updated by combining $state_0$ and the candidate value a_t , modulated by the forget f_t and input i_t gates as described in equation (5). The updated cell state retains long-term dependencies critical for understanding trends in evapotranspiration.

$$state_t = (a_t \odot i_t + f_t \odot state_0) \quad (5)$$

Where \odot represents the element-wise product called Hadamard product, $state_t$ represents the new state, and $state_0$ represents the previous state.

The output gate determines the hidden state out_t to be passed to the next cell and used for predictions. It involves two steps, which are equation (6) and (7).

The output of equation (7) is the hidden state out_t . It represents the processed information at the current time step. It therefore passed to a fully connected layer to generate the predicted evapotranspiration value(s) for future time steps.

$$o_t = \sigma(W_o \cdot x_t + U_o \cdot out_0 + b_o) \quad (6)$$

$$out_t = \tanh(state_t) \odot o_t \quad (7)$$

where out_t represents the hidden vector of the LSTM unit.

The LSTM architecture for this study consists of 2 LSTM layers, a dense layer, and output layer. LSTM layer 1 accepts an input shape: (n_input , $n_features$) = (30, 1) and 50 LSTM units. n_input Represents the number of time steps in the input sequence. This indicates how many historical times steps the model considers when making a prediction. For instance, for the model to forecast a day evapotranspiration value; the model will use data from the past 30 days. $n_features$ represents the number of features (variables) available for each time step. In the context of this research, the data used is univariate and the feature is the evapotranspiration value. LSTM layer 2 accept input from the first LSTM layer with shape: (n_input , units) = (30, 50). These will output a single time step vector of shape 50. Dense Layer takes the 50 outputs from the second LSTM layer and produces 25 outputs. Output Layer takes 25 inputs from the dense layer and outputs a single value for regression. Figure 6 shows the summary of LSTM architecture.

Model: "sequential"

Layer (type)	Output Shape	Param #
lstm (LSTM)	(None, 30, 50)	10,400
lstm_1 (LSTM)	(None, 50)	20,200
dense (Dense)	(None, 25)	1,275
dense_1 (Dense)	(None, 1)	26

Total params: 31,901 (124.61 KB)
 Trainable params: 31,901 (124.61 KB)
 Non-trainable params: 0 (0.00 B)

Fig 6 Summary of LSTM Architecture

E. Comparative Models

Convolutional Neural Network (CNN) are a class of deep learning models designed primarily for processing structured grid-like data, such as images and time series. They use convolutional layers to automatically extract spatial and temporal features, reducing the need for manual feature engineering. CNNs have revolutionized fields like computer vision, but their adaptability extends beyond image analysis. In the context of evapotranspiration forecasting, CNNs can be employed to analyze temporal patterns in meteorological data. By capturing intricate dependencies within historical climate variables such as temperature, humidity, windspeed, and solar radiation, CNNs can learn complex relationships that influence evapotranspiration rates. Unlike traditional models that rely on predefined equations, CNNs leverage data-driven learning, making them effective in handling nonlinear variations in weather patterns.

Artificial Neural Network (ANN) Conventional ANN consists of multiple layers of neurons, including an input layer, hidden layers, and an output layer. In evapotranspiration forecasting, ANN maps meteorological input features to predict evapotranspiration (ET) values. Each neuron in the hidden layer performs a weighted sum of the inputs, adds a bias, and applies an activation function.

Gated Recurrent Unit (GRU) is a variant of RNN designed to address the vanishing gradient problem in standard RNNs. Its ability to model temporal dependencies makes it suitable for predicting ET. Given an input feature vector which include temporal features derived from date, the GRU updates its hidden state h_t at each time step using the following equations:

$$z_t = (W_z[h_{t-1}, x_t] + b_z) \quad (8)$$

$$r_t = (W_r[h_{t-1}, x_t] + b_r) \quad (9)$$

$$\tilde{h} = \tanh(W_{\tilde{h}}[r_t \odot h_{t-1}, x_t] + b_{\tilde{h}}) \quad (10)$$

Where W_z , W_r , and $W_{\tilde{h}}$ are weight matrix for update z_t , reset r_t , and candidate hidden state \tilde{h}_t respectively, b_z , b_r , $b_{\tilde{h}}$ are the bias terms, σ is the sigmoid activation, h_{t-1} is the past hidden state, and \odot is element-wise multiplication.

➤ Bi-Directional GRU:

The Bi-GRU is a type of recurrent neural network (RNN) architecture that extends the standard GRU by incorporating bidirectional processing. Unlike traditional GRUs, which process data in a single direction (past to future), Bi-GRUs utilize two GRU layers one reading the sequence forward and the other in reverse. This dual processing enables the model to capture both past and future dependencies, making it more effective for sequence learning tasks such as time series forecasting, speech recognition, and natural language processing. In evapotranspiration prediction, Bi-GRU improves forecasting accuracy by

leveraging both past weather trends and potential future influences within historical data. This ability allows for better handling of complex, nonlinear relationships in climate patterns, enhancing water resource management and agricultural planning.

➤ Bi-Directional LSTM Network:

The Bi-LSTM network is a variant of the LSTM model that processes input sequences in both forward and backward directions. LSTMs are known for their ability to retain long-term dependencies, addressing the vanishing gradient problem in traditional RNNs. By incorporating bidirectionality, Bi-LSTMs gain a more comprehensive understanding of sequence dynamics, making them particularly useful for forecasting problems where both past and future context are essential.

F. Performance Metrics

Mean Squared Error (MSE) measures the average of the squared differences between predicted and actual values. It is a widely used metric for regression tasks because it emphasizes larger errors due to the squaring operation, making it sensitive to outliers.

$$MSE = \frac{1}{n} \sum_{i=1}^n (y_i - \hat{y}_i)^2 \quad (11)$$

where n is the number of evapotranspiration samples, y_i is actual value, and \hat{y}_i is the predicted value

Root Mean Squared Error (RMSE) is the square root of the MSE. It provides an interpretable measure of error in the same units as the target variable, making it more intuitive than MSE.

$$RMSE = \sqrt{\frac{1}{n} \sum_{i=1}^n (y_i - \hat{y}_i)^2} \quad (12)$$

Mean Absolute Error (MAE) measures the average magnitude of errors between predicted and actual values, ignoring their direction. It provides a straightforward interpretation of the average error.

$$MAE = \frac{1}{n} \sum_{i=1}^n |y_i - \hat{y}_i| \quad (13)$$

➤ Experimental Setup

The system was developed using the Python programming language, leveraging various Python libraries essential for deep learning implementation. These libraries include Keras for model development, NumPy and Pandas for data manipulation, Matplotlib for visualization, and Scikit-learn for data preprocessing and evaluation. For the development environment, Google Colaboratory was chosen as the primary platform due to its accessibility, cloud-based GPU support, and integration with Google Drive for seamless data storage and retrieval.

IV. RESULTS AND DISCUSSION

A. Daily Evapotranspiration

A detailed evaluation of the LSTM model's performance is presented, comparing the predicted values with actual ET measurements as well as presenting the performance of the model based on standard metrics. Table 3 provides a comprehensive comparison between observed and predicted values, offering insights into the model's predictive accuracy.

Table 3 Actual value and predicted LSTM values

Date	Actual Value	LSTM Pred
2023-12-03	5.6	5.953311
2023-12-04	5.5	5.872607
2023-12-05	5.5	5.780755
2023-12-06	5.9	5.748665
2023-12-07	5.0	5.981606
2023-12-08	5.8	5.469844
2023-12-09	5.6	5.834097
2023-12-10	5.6	5.778281
2023-12-11	5.6	5.756358
2023-12-12	5.9	5.746358
2023-12-13	5.8	5.926386
2023-12-14	5.8	5.896386
2023-12-15	5.6	5.888851
2023-12-16	5.6	5.762726
2023-12-17	5.6	5.733296
2023-12-18	5.7	5.723642
2023-12-19	5.0	5.779881
2023-12-20	5.4	5.364153
2023-12-21	5.2	5.504023
2023-12-22	5.6	5.408725



Fig 7 The Graphical Representation of the Daily Actual, Validation, and LSTM predicted values

Based on Table 3, the predicted values from the LSTM model are consistently close to the actual evapotranspiration values, indicating that the model has successfully learned the underlying patterns in the dataset. The deviations between the actual and predicted values are generally small, typically within a range of approximately ± 0.6 units. This suggests the model has a good fit to the data. On dates like 2023-12-03, 2023-12-04, and 2023-12-11, the predicted values (e.g., 5.953311, 5.872607, and 5.756358) are very close to the actual values (5.6, 5.5, and 5.6, respectively). Such results demonstrate the model's ability to effectively generalize and predict future data points. However, there are

some notable deviations. On 2023-12-08, the actual evapotranspiration value is 5.8, while the predicted value is significantly lower at 5.469844. This represents a deviation of approximately -0.33 units. Similarly, on 2023-12-19, the actual value is 5.0, while the predicted value is 5.779881, showing a deviation of +0.78 units.

Figure 8 shows the plot for training, validation, and the LSTM prediction of daily data, while Table 4 presents the evaluation result for LSTM prediction on the daily evapotranspiration task.

Table 4 LSTM Evaluation on Daily test data

Metrics	value
Accuracy	0.9568
MSE	0.0034
RMSE	0.0583
MAE	0.0433

➤ *Accuracy (0.9568):*

The value of 0.9568 is very high, suggesting that the model is performed well in making predictions relative to the true values.

- The MSE of 0.0034 is quite low, which is a good sign of accuracy and precision in the model's predictions.
- The RMSE value of 0.0583 suggests that, on average, the model's predictions deviate from the actual values by approximately 0.0583 units. A small RMSE indicates that the model's predictions are very close to the actual values.
- An MAE of 0.0433 is also quite low, suggesting that the

model's predictions are typically off by only about 0.0433 units on average, which is a good result.

Overall Assessment shows that the model is performed excellently, with high accuracy and low error values across the board. Specifically, an accuracy of 95.68% and low values for MSE, RMSE, and MAE suggest that the model is highly accurate and precise in making predictions. Table 5 presents the LSTM daily forecasted values, while Figure 9 displays the graphical representation of the daily forecasted values.

Table 5 LSTM Daily Forecasted Values

Date	LSTM Forecast value
2023-12-23	5.625234
2023-12-24	5.683219
2023-12-25	5.730966
2023-12-26	5.772871
2023-12-27	5.810213
2023-12-28	5.844479
2023-12-29	5.876368
2023-12-30	5.906655
2023-12-31	5.936096
2023-01-01	5.965177
2023-01-02	5.994234
2023-01-03	6.023552
2023-01-04	6.053301
2023-01-05	6.083535
2023-01-06	6.114115
2023-01-07	6.145453
2023-01-08	6.177037
2023-01-09	6.209017
2023-01-10	6.241320
2023-01-11	6.273898

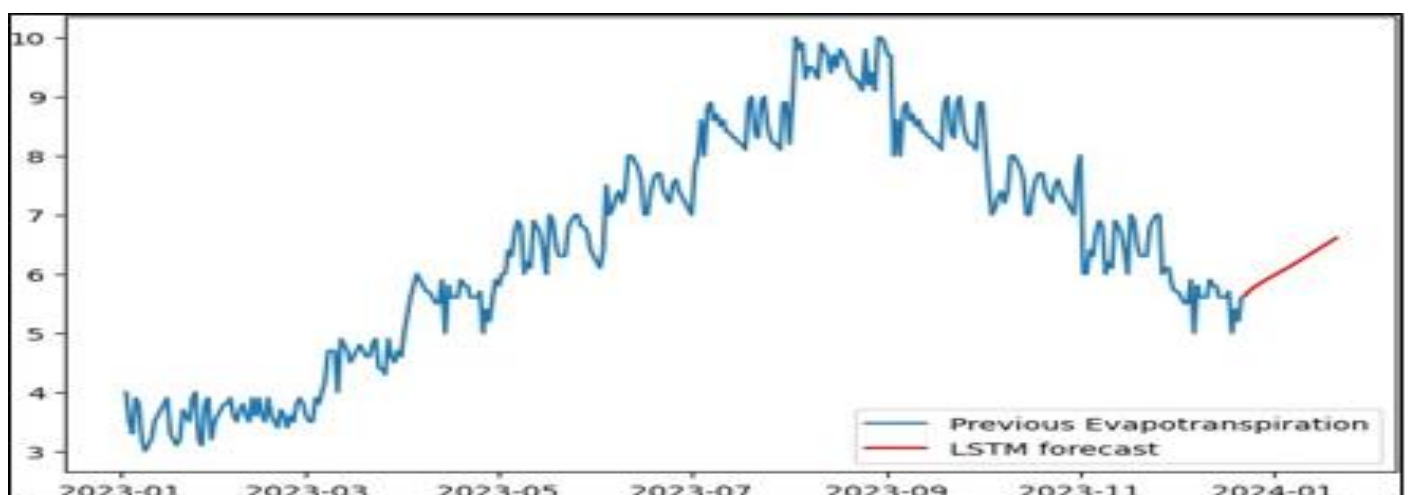


Fig 8 The Graphical Representation of the Daily Forecasted value

V. PERFORMANCE COMPARISON WITH OTHER COMPARATIVE MODELS

A. Mid Term Evapotranspiration (Daily model)

The Figure 9 shows the training loss trends of the comparative models (ANN, GRU, Bi-LSTM, Bi-GRU, CNN) including, LSTM over 50 epochs, highlighting their convergence patterns and stability. ANN Starts with high loss, drops rapidly within 5 epochs, stabilizes after ~15 epochs with minor fluctuations, achieving low final loss. GRU Sharp initial decline but more fluctuations than ANN; stabilizes around 15 epochs, ending with steady low loss. Bi-LSTM Slightly higher initial loss than others but stabilizes smoothly after a rapid early drop, achieving the lowest final loss with consistency (top performer). Bi-GRU Similar early loss reduction to Bi-LSTM but with more fluctuations before stabilizing (10–15 epochs); final loss comparable to GRU. CNN Exhibits persistent fluctuations throughout training, gradual decline, and less stability than recurrent models, yet achieves a low (albeit less smooth) final loss. LSTM Starts with the highest initial loss, declines sharply early, stabilizes with occasional fluctuations, and ends with low, stable loss.

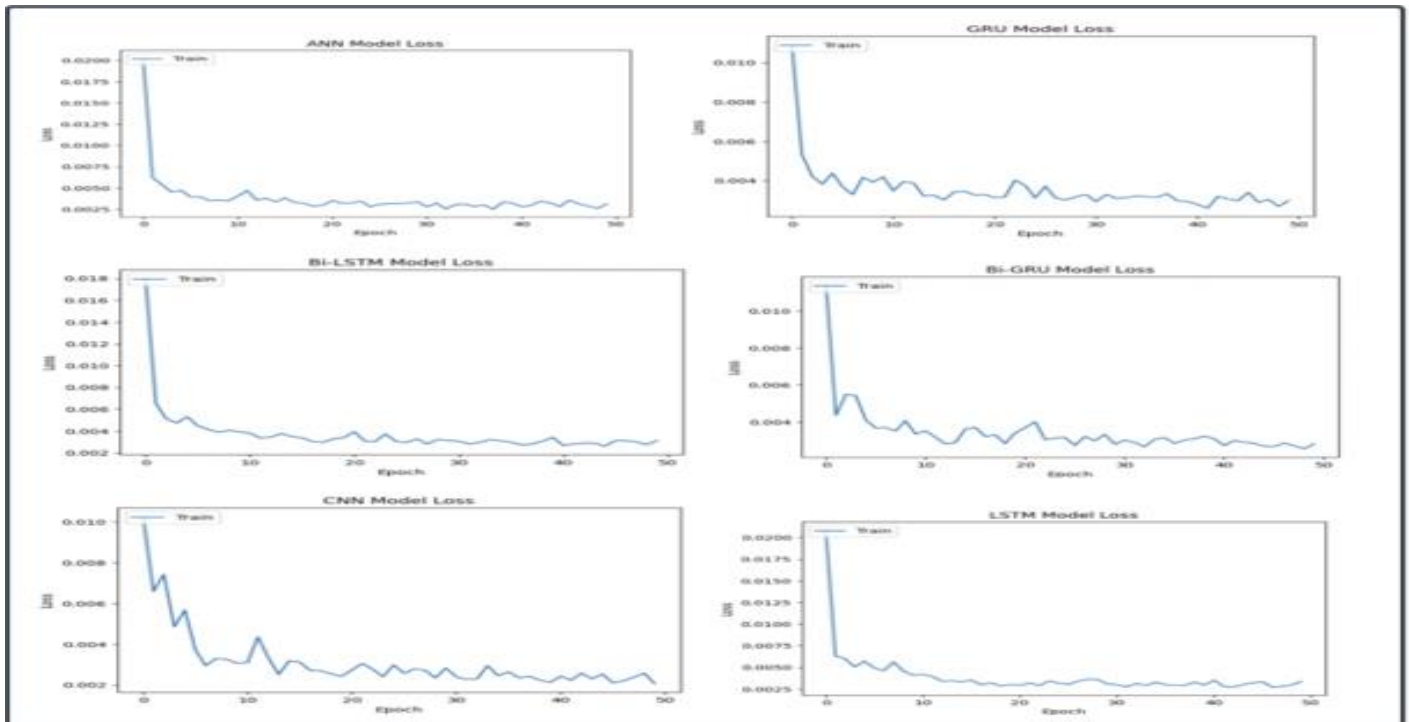


Fig 9 Models Loss for Daily Training Data

Table 6 Comparative Predictions of Daily Evapotranspiration

Date	Actual Value	LSTM Pred	CNN Pred	GRU Pred	ANN Pred	Bi-LSTM Pred	Bi-GRU Pred
2023-12-03	5.6	5.953311	5.934629	6.007970	6.269683	6.159265	6.149006
2023-12-04	5.5	5.872607	5.906876	5.909600	6.245405	6.089574	6.097361
2023-12-05	5.5	5.780755	6.261494	5.808281	6.257376	6.005129	6.007585
2023-12-06	5.9	5.748665	6.208382	5.783804	6.274242	5.946955	5.890897
2023-12-07	5.0	5.981606	6.176565	6.048241	6.219503	6.141411	6.043536
2023-12-08	5.8	5.469844	5.761432	5.490928	5.999240	5.666285	5.579797
2023-12-09	5.6	5.834097	5.837838	5.905838	6.200474	6.054063	6.049279
2023-12-10	5.6	5.778281	6.042766	5.883103	6.299156	6.034836	6.145674
2023-12-11	5.6	5.756358	5.891913	5.756944	6.207011	6.030442	6.005251
2023-12-12	5.9	5.746358	5.908746	5.834259	6.103436	5.992534	5.964360
2023-12-13	5.8	5.926386	6.131533	6.007602	6.224924	6.155228	6.122394
2023-12-14	5.8	5.896386	6.074751	5.980446	6.231280	6.137808	6.143321
2023-12-15	5.6	5.888851	6.251398	5.954283	6.230247	6.154355	6.217968
2023-12-16	5.6	5.762726	6.185749	5.851364	6.315797	6.049516	6.106822
2023-12-17	5.6	5.733296	5.899385	5.821526	6.215755	5.982413	5.953863
2023-12-18	5.7	5.723642	5.926521	5.836035	6.183595	5.969590	5.929897
2023-12-19	5.0	5.779881	5.960268	5.885684	6.260021	6.051025	6.005068
2023-12-20	5.4	5.364153	5.659458	5.441394	5.978889	5.694838	5.664302
2023-12-21	5.2	5.504023	5.583258	5.610387	6.119390	5.857392	5.874679
2023-12-22	5.6	5.408725	5.741256	5.538786	6.026420	5.784208	5.852827

According to Table 6, LSTM exhibited the best predictive accuracy, consistently maintaining values close to the actual ET measurements. For instance, on December 3, 2023, the actual ET was 5.6, and the LSTM prediction was 5.95, demonstrating a minor overestimation. Across multiple dates, LSTM predictions remained stable with relatively low variance, highlighting its ability to capture sequential dependencies effectively. However, it exhibited slight underestimations on certain dates (December 12, where the actual ET was 5.9, and LSTM predicted 5.74).

CNN demonstrated higher variance in predictions, occasionally deviating more than recurrent models. For instance, on December 5, the CNN prediction (6.26) overestimated the actual ET (5.5) significantly. This tendency suggests that CNN may struggle with capturing temporal dependencies as effectively as LSTM.

GRU also performed well in capturing ET trends. On December 3, the GRU-predicted value (6.00) closely matched the actual value (5.6), indicating strong forecasting ability. However, slight overestimations were observed, particularly on December 7, where the predicted ET (6.04)

exceeded the actual value (5.0). Overall, GRU maintained a balance between accuracy and computational efficiency, making it a strong alternative to LSTM.

The ANN model exhibited the largest deviations from actual values across multiple instances. On December 3, ANN predicted 6.27, an overestimation of nearly 0.7 units. Similar overestimations were seen on December 7 (6.21 against 5.0) and December 10 (6.30 against 5.6). These results suggest that ANN struggled to capture temporal dependencies effectively, making it less reliable for ET forecasting compared to recurrent architectures.

➤ *Bi-LSTM and Bi-GRU Model Performance*

Bidirectional variants of LSTM and GRU, Bi-LSTM and Bi-GRU, provided competitive results, leveraging information from both past and future time steps. These models generally followed the trends observed in LSTM and GRU but introduced slight smoothing effects. On December 5, Bi-LSTM predicted 6.00, closer to the actual ET (5.5) than CNN (6.26). Figure 10 shows the graphical representation of the comparative predictions of the Models for daily evapotranspiration

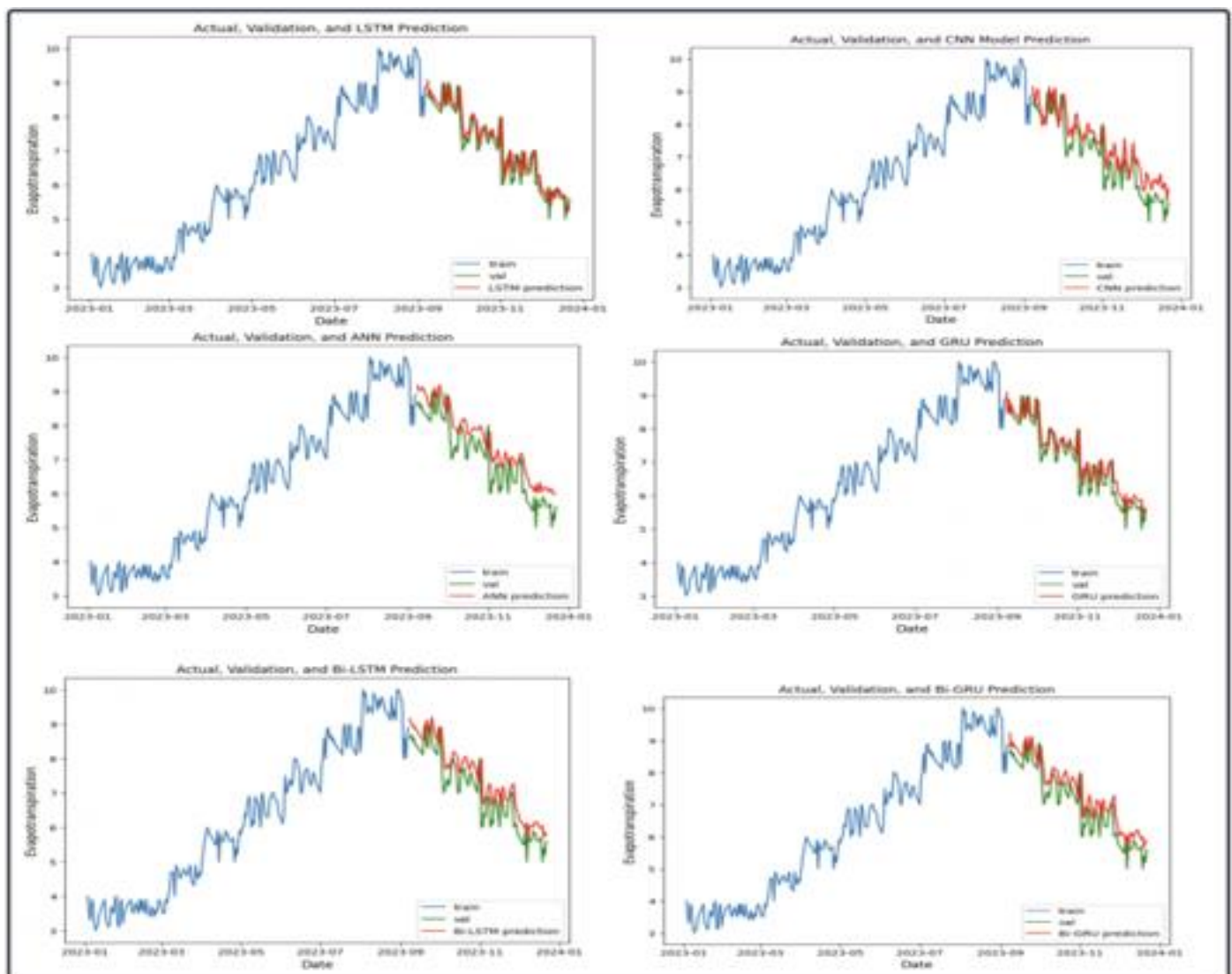


Fig 10 The Graphical Representation of the Actual, Validation of the Models Daily predicted values

Table 7 Performance Comparison on Daily Evapotranspiration Data

Metrics	LSTM	CNN	ANN	GRU	Bi-LSTM	Bi-GRU
Accuracy	0.9568	0.9330	0.9180	0.9508	0.9323	0.93722
MSE	0.0034	0.0068	0.0089	0.0036	0.0064	0.00566
RMSE	0.0583	0.0825	0.0094	0.0605	0.0798	0.07528
MAE	0.0433	0.0673	0.0823	0.0451	0.0679	0.06306

Table 7 presents the comparison of LSTM, CNN, GRU, Bi-LSTM, Bi-GRU, and ANN models for daily ET prediction. Among the models evaluated, LSTM demonstrates the highest accuracy (0.9568), making it the most effective for capturing temporal dependencies in ET data. GRU follows closely with an accuracy of 0.9508, indicating that it also performs well in modeling sequential patterns. On the other hand, ANN has the lowest accuracy (0.9180), suggesting that it struggles to learn the complex relationships governing evapotranspiration. Meanwhile, CNN (0.9330), Bi-LSTM (0.9323), and Bi-GRU (0.9372) exhibit moderate performance, but they do not match the precision of LSTM and GRU. When considering the MSE, LSTM achieves the lowest value (0.0034), followed closely by GRU (0.0036), indicating minimal deviation from actual ET values. In contrast, ANN records the highest MSE (0.0089), reinforcing its weaker predictive performance. The MSE values for CNN (0.0068), Bi-LSTM (0.0064), and Bi-GRU (0.00566) are notably higher than those of LSTM and GRU, confirming that these models introduce more errors in their predictions.

A similar trend is observed in RMSE, where LSTM records the lowest RMSE (0.0583), making it the most precise model, with GRU slightly behind at 0.0605. On the other hand, CNN (0.0825), Bi-LSTM (0.0798), and Bi-GRU (0.07528) exhibit considerably higher RMSE values, indicating greater variability in their predictions. These results suggest that LSTM and GRU provide more stable and accurate ET estimates, while CNN and Bi-LSTM introduce greater inconsistencies.

MAE values further highlight LSTM's superiority, as it achieves the lowest MAE (0.0433), followed closely by GRU (0.0451). This indicates that these two models have the smallest absolute prediction errors on average. In contrast, ANN again performs the worst, with the highest MAE (0.0823), further confirming its struggles in accurately predicting ET values. Similarly, CNN (0.0673), Bi-LSTM (0.0679), and Bi-GRU (0.06306) exhibit higher MAE values, reinforcing the observation that these models are less reliable than LSTM and GRU.

Overall, LSTM emerges as the best-performing model for daily evapotranspiration prediction, achieving the highest accuracy and the lowest error metrics across all evaluations. GRU proves to be a strong alternative, offering nearly comparable performance with slightly higher error values. Meanwhile, ANN exhibits the weakest performance, struggling with the lowest accuracy and the highest errors. The results also indicate that CNN, Bi-LSTM, and Bi-GRU provide moderate performance but introduce more errors than LSTM and GRU.

B. Monthly Evapotranspiration

The Table 8 presents a comparison between actual evapotranspiration values and LSTM-predicted values over a period spanning from May 2003 to December 2004. The evaluation of the predicted values in relation to the actual values helps in assessing the performance LSTM model for evapotranspiration forecasting.

Table 8 Monthly Actual value and predicted LSTM values

Date	ActualData	LSTMPrediction
2003-05-01	201.9	200.868698
2003-06-01	216.5	216.501877
2003-07-01	228.9	228.193863
2003-08-01	223.9	223.944763
2003-09-01	207.9	207.941879
2003-10-01	185.9	185.966797
2003-11-01	172.1	167.576508
2003-12-01	160.3	153.764572
2004-01-01	142.2	144.295288
2004-02-01	150.5	150.239685
2004-03-01	166.8	166.705338
2004-04-01	184.2	184.614059
2004-05-01	204.8	202.009293
2004-06-01	220.1	218.166992
2004-07-01	233.2	228.869125
2004-08-01	227.8	224.771118
2004-09-01	212.3	210.885864
2004-10-01	191.2	189.121323

2004-11-01	168.5	167.002701
2004-12-01	153.9	155.540787

Based on Table 8, LSTM's predictions closely align with actual evapotranspiration (ET) measurements. In June 2003, the model's prediction (216.50 mm) matches the observed ET value (216.5 mm), reflecting its ability to capture the sustained ET levels during the peak rainy season. Whilesolar radiation is reduced due to persistent cloud cover, high soil moisture and relative humidity sustain evapotranspiration, particularly during short breaks in rainfall. Similarly, in March 2004, the prediction(166.71 mm) is almost identical to the actual value (166.8 mm), indicating the model effectively tracks the seasonal rebound in ET as the dry season transitions into the rainy season, when rising humidity and increasing soil moisture promote higher ET rates. These results highlight the LSTM's capability to model seasonal hydrological cycles, which are critical for water resource management, irrigation planning, and ecosystem studies.

However, discrepancies emerge during periods of abrupt environmental change. In November 2003, the model underestimates ET by 4.5 mm (predicted 167.58 mm against actual 172.1 mm). This could reflect residual soil moisture from late-season rains, which sustains ET longer than expected, or a delay in seasonal cooling that the LSTM does not fully capture. Similarly, in December 2003, the gap widens to 6.5 mm (153.76 mm against 160.3 mm), potentially due to localized climatic variations such as unseasonably warm conditions or delayed vegetation dormancy, both of which sustain higher ET rates. These errors underscore the challenge of modeling ET during transitional months, where complex interactions between meteorology, soil moisture, and land cover disrupt typical seasonal patterns.

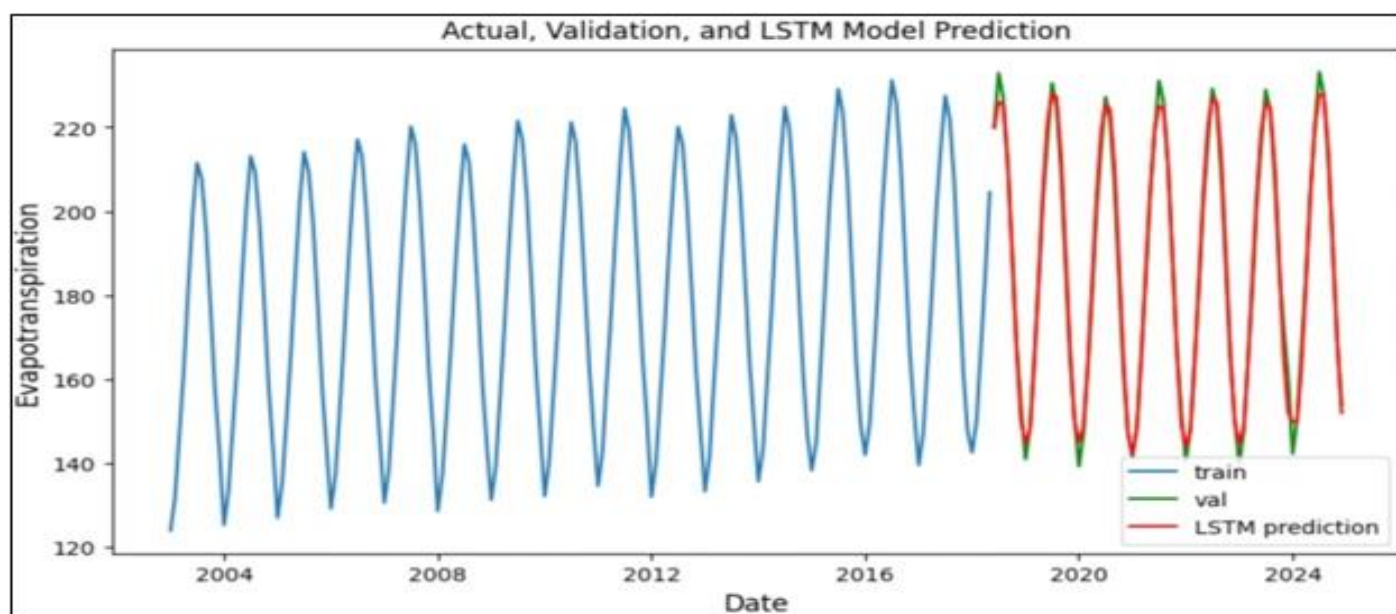


Fig 11 The Graphical Representation of the Monthly Actual, Validation, LSTM predicted values

Table 9 LSTM Evaluation on Monthly test data

Metrics	Value
Accuracy	0.9894
MSE	0.0005
RMSE	0.0222
MAE	0.0182

The Table 9 presents the overall performance evaluation of the LSTM model using standard statistical metrics:

➤ **Accuracy (0.9894):**

Indicates a high level of agreement between predicted and actual values, demonstrating strong model performance.

➤ **Mean Squared Error (MSE: 0.0005):**

A very low value, signifying minimal error in the model's predictions.

➤ **Root Mean Squared Error (RMSE: 0.0222):**

Reinforces the reliability of the model by showing that the average error remains low.

➤ **Mean Absolute Error (MAE: 0.0182):**

Suggests that the model's predictions deviate only slightly from actual values on average.

Table 10 LSTM Monthly Forecast Values

Date	LSTM Forecast value
2025-01-01	141.929281
2025-02-01	145.657203
2025-03-01	158.423081
2025-04-01	176.444225
2025-05-01	196.111431
2025-06-01	213.586176
2025-07-01	224.086926
2025-08-01	223.452575
2025-09-01	211.240117
2025-10-01	191.138596
2025-11-01	168.555804
2025-12-01	149.373704
2026-01-01	139.542873
2026-02-01	141.816560
2026-03-01	154.003449
2026-04-01	171.989765
2026-05-01	192.015734
2026-06-01	210.298443
2026-07-01	222.097408
2026-08-01	222.946363

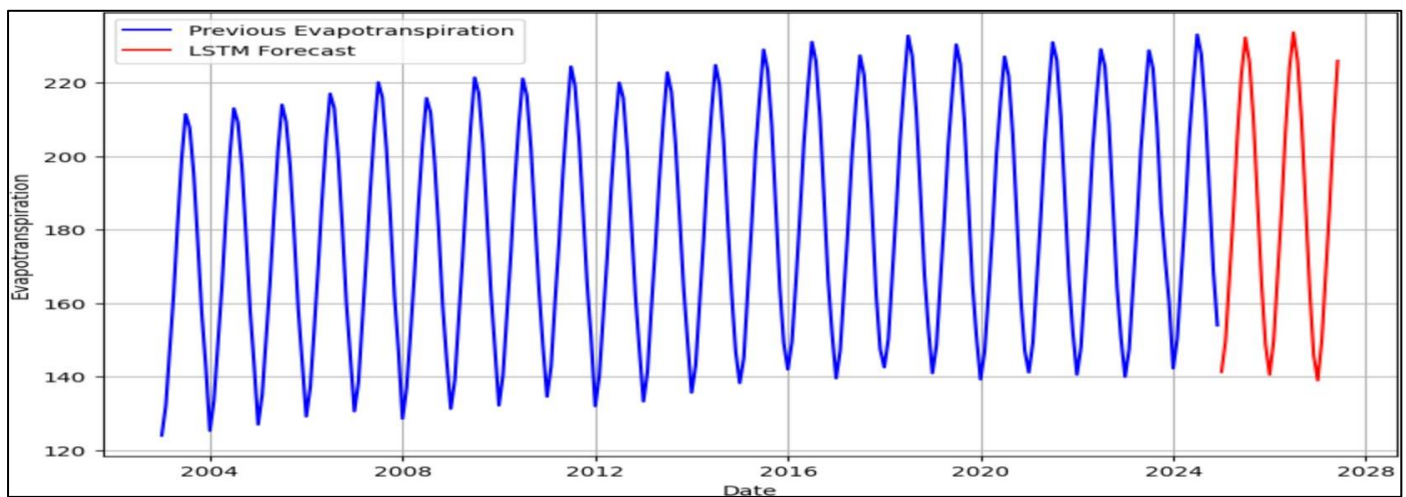


Fig 12 The Graphical Representation of the Monthly Forecasted value

Table 11 Comparative Predictions of Monthly Evapotranspiration

Date	ActualData	LSTM Prediction	GRU Prediction	Bi-LSTM Prediction	Bi-GRU Prediction	CNN Prediction	ANN Prediction
2003-05-01	201.9	200.868698	203.602234	201.735077	206.582993	196.577759	198.859253
2003-06-01	216.5	216.501877	221.342545	216.026337	221.538193	212.414581	215.302444
2003-07-01	228.9	228.193863	226.688339	221.992828	226.096039	221.930176	221.897156
2003-08-01	223.9	223.944763	224.959717	218.825928	223.081894	220.137772	219.255463
2003-09-01	207.9	207.941879	207.490311	203.803162	204.421295	206.423813	205.155624
2003-10-01	185.9	185.966797	186.793915	182.619202	181.814346	186.590195	183.952805
2003-11-01	172.1	167.576508	165.549896	160.442627	157.933594	165.445312	161.615585
2003-12-01	160.3	153.764572	154.182617	146.273468	144.623703	153.557266	147.890121
2004-01-01	142.2	144.295288	150.682877	141.004562	139.488892	146.606522	144.904617
2004-02-01	150.5	150.239685	151.275253	144.886459	143.107376	148.459198	146.519928
2004-03-01	166.8	166.705338	166.724289	160.507874	162.467545	162.743515	158.765366
2004-04-01	184.2	184.614059	185.849197	181.091156	185.069138	178.714722	178.214264
2004-05-01	204.8	202.009293	204.631775	200.618591	205.202957	198.094421	198.531387
2004-06-01	220.1	218.166992	222.814423	216.116165	221.467606	213.568604	215.791794
2004-07-01	233.2	228.869125	229.126358	223.995392	227.881546	223.387558	223.770767

2004-08-01	227.8	224.771118	228.444733	221.184891	225.327164	222.570740	222.562134
2004-09-01	212.3	210.885864	210.455276	205.824554	206.097260	208.737457	208.956100
2004-10-01	191.2	189.121323	190.557861	184.733856	184.055191	189.408859	187.97724
2004-11-01	168.5	167.002701	170.163101	162.961929	160.695465	168.475082	165.972778
2004-12-01	153.9	155.540787	151.220520	146.512299	143.332657	153.871231	148.517456

According to Table 11, the actual ET data follows a distinct seasonal cycle, peaking in mid-year months (i.e., July 2003: 228.9 mm; July 2004: 233.2 mm) and dipping in harmattan (January 2004: 142.2 mm), reflecting typical evapotranspiration dynamics driven by temperature, sunlight, and vegetation activity. Most models track this seasonal trend but differ in their precision:

LSTM and GRU predictions align closely with actual values during stable periods (June 2003: LSTM predicts 216.50 against actual 216.5; GRU predicts 221.34).

Bi-GRU and Bi-LSTM (bidirectional models) occasionally lag behind peaks, such as in July 2003, where Bi-LSTM predicts 221.99 mm against the actual 228.9 mm,

suggesting challenges in capturing rapid wet season increases.

CNN and ANN show mixed results, with CNN consistently underestimating peaks (i.e., July 2004: CNN predicts 223.39 against actual 233.2) and ANN struggling with harmattan (i.e., January 2004: ANN predicts 144.90 against the actual 142.2).

Conclusively, all the models capture the broad seasonal ET cycle, their performance varies significantly during critical periods. GRU and LSTM strike the best balance between accuracy and robustness, but bidirectional architectures and CNNs lag in peak seasons.

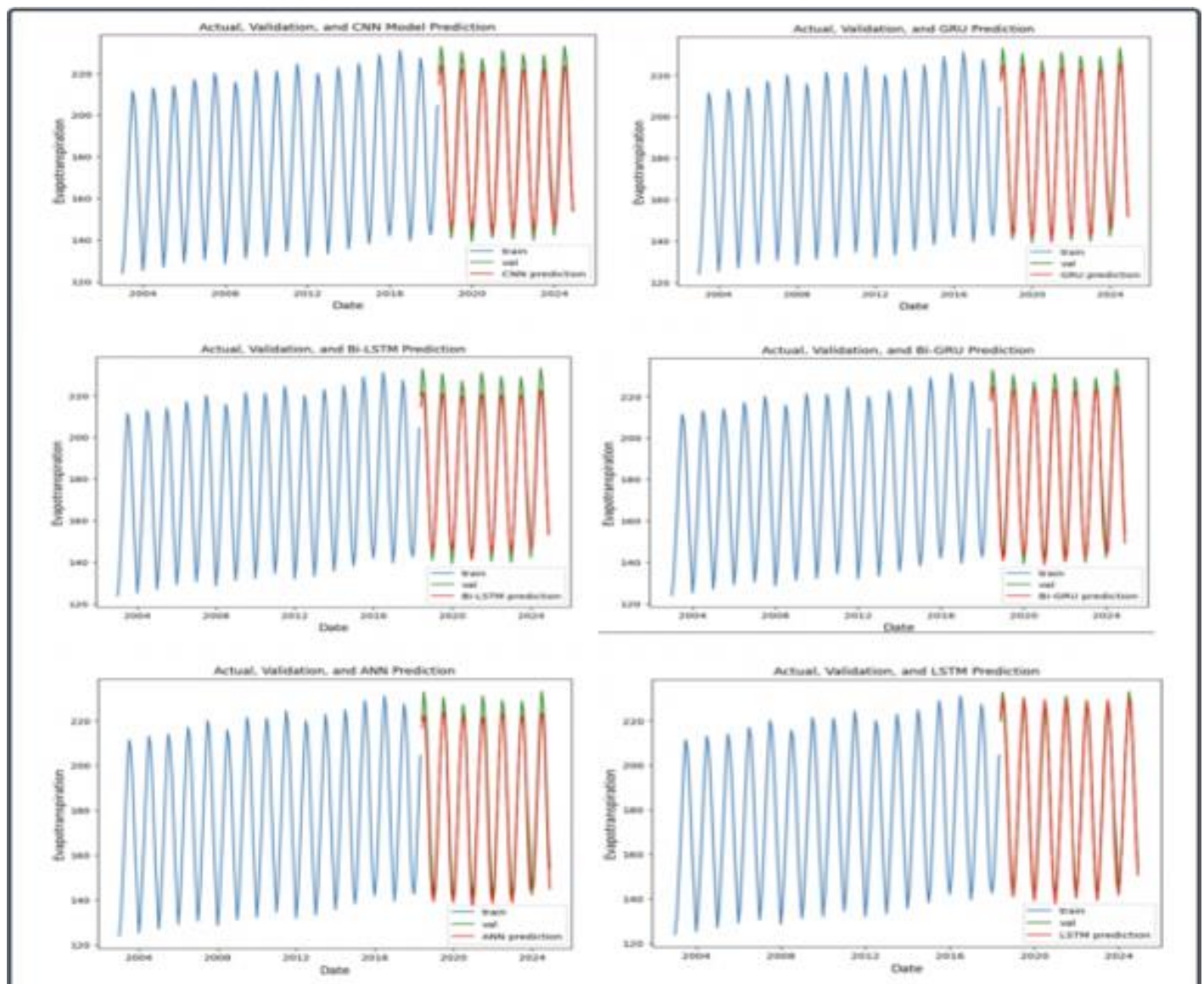


Fig 13 The Graphical Representation of the Actual, Validation of the Models Monthly predicted values

Table 12 Performance comparison on Monthly Data

Metrics	LSTM	CNN	ANN	GRU	Bi-LSTM	Bi-GRU
Accuracy	0.9894	0.9782	0.9779	0.9860	0.97492	0.9758
MSE	0.0005	0.0016	0.0019	0.0008	0.00244	0.0025
RMSE	0.0222	0.0431	0.0446	0.0287	0.04289	0.0504
MAE	0.0182	0.0385	0.0377	0.0229	0.04289	0.0412

Based on Table 12, the LSTM model emerged as the most accurate and reliable predictor of evapotranspiration, achieving a near-perfect accuracy score of 0.9894 and the lowest error rates across all metrics. With a MSE of 0.0005 and a RMSE of 0.0222. Its minimal mean absolute error (MAE) of 0.0182 mm further buttressed its precision, making it an ideal choice for evapotranspiration.

The GRU model trailed closely behind LSTM, with an

In contrast, CNN and ANN models delivered mid-tier results, with accuracies hovering around 0.978 and RMSE values nearing 0.04. These models struggled to match the temporal sophistication of LSTM and GRU. The CNN, designed primarily for spatial data, appeared ill-suited to the sequential nature of ET time series, while the ANN's lack of built-in mechanisms to handle time-dependent relationships limited its ability to resolve seasonal trends. Their higher errors particularly in capturing peak ET values during dry season months highlighted their limitations in forecasting, where temporal context is critical. Surprisingly, bidirectional architectures like Bi-LSTM and Bi-GRU underperformed despite their theoretical promise. With accuracies below 0.976 and RMSE values exceeding 0.04, these models lagged significantly behind their unidirectional counterparts. This unexpected result may stem from their bidirectional design, which processes data both forward and backward in time a feature better suited to tasks like language modeling, where future context is meaningful.

VI. WEB APP DEVELOPMENT

To ensure seamless deployment and scalability, the application utilizes Dockerization for model deployment. Docker provides a containerized environment that packages the model, application code, and dependencies into a single portable unit. This approach ensures that the application runs consistently across different systems and simplifies the process of sharing and updating the software. The Dockerized application is deployed on a local drive, providing easy access and cost-effective operation for local users without reliance on cloud services.

A suitability range was provided for various crops to guide planting decisions by agronomists. The suitability insight is dynamically highlighted based on user-selected crops, enabling farmers to easily determine if the forecasted evapotranspiration is suitable for optimal growth and productivity. Forecast data is displayed in easy-to-read tabular formats, ensuring that farmers and stakeholders in Ogwashi-Uku can quickly interpret and apply the information. These ranges, derived from agronomic best

accuracy of 0.9860 and marginally higher errors (MSE: 0.0008, RMSE: 0.0287). While its simplified architecture likely reduced computational overhead, the slight trade-off in precision suggests GRU may occasionally overlook nuanced patterns that LSTM's more complex memory cells can retain. Still, its strong performance positions it as a practical alternative for scenarios where computational efficiency is prioritized without sacrificing significant accuracy.

practices, are presented as follows:

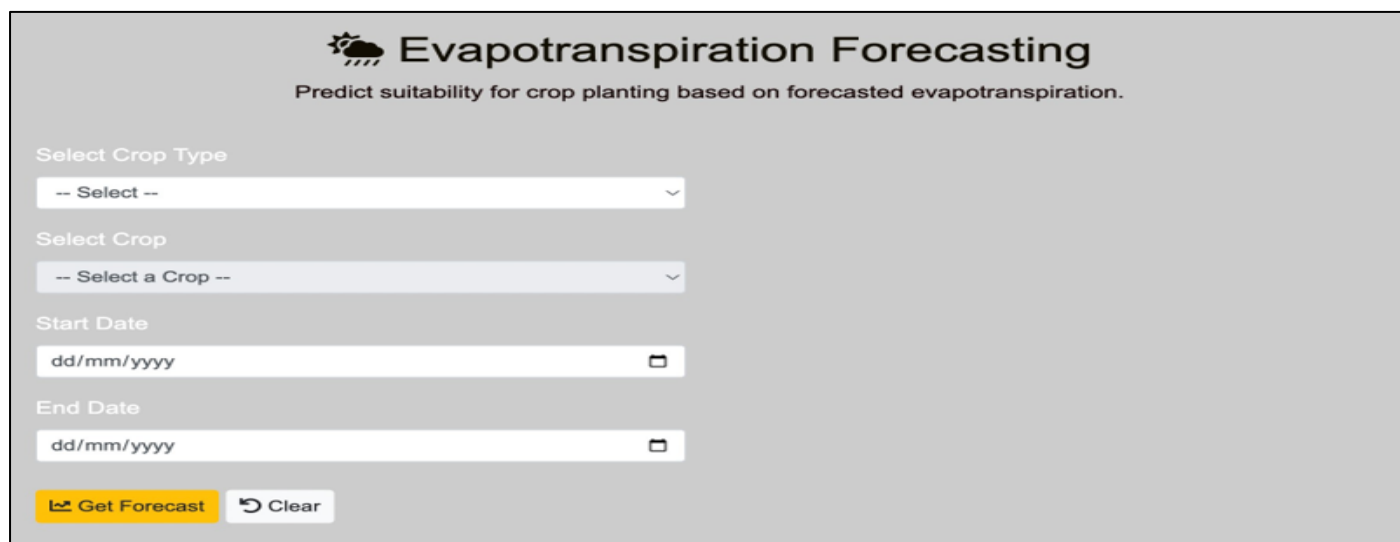
➤ Food Crops:

- Maize (Corn): 4.5-6.5 mm/day
- Cassava: 4.0-6.0 mm/day
- Yam: 3.5-5.5 mm/day
- Rice: 5.0-7.0 mm/day
- Vegetables (e.g., Tomatoes, Peppers): 4.0-6.0 mm/day
- Okra: 3.5-5.5 mm/day
- Cowpea: 3.5-5.5 mm/day
- Plantain: 4.5-6.5 mm/day

➤ Cash Crops:

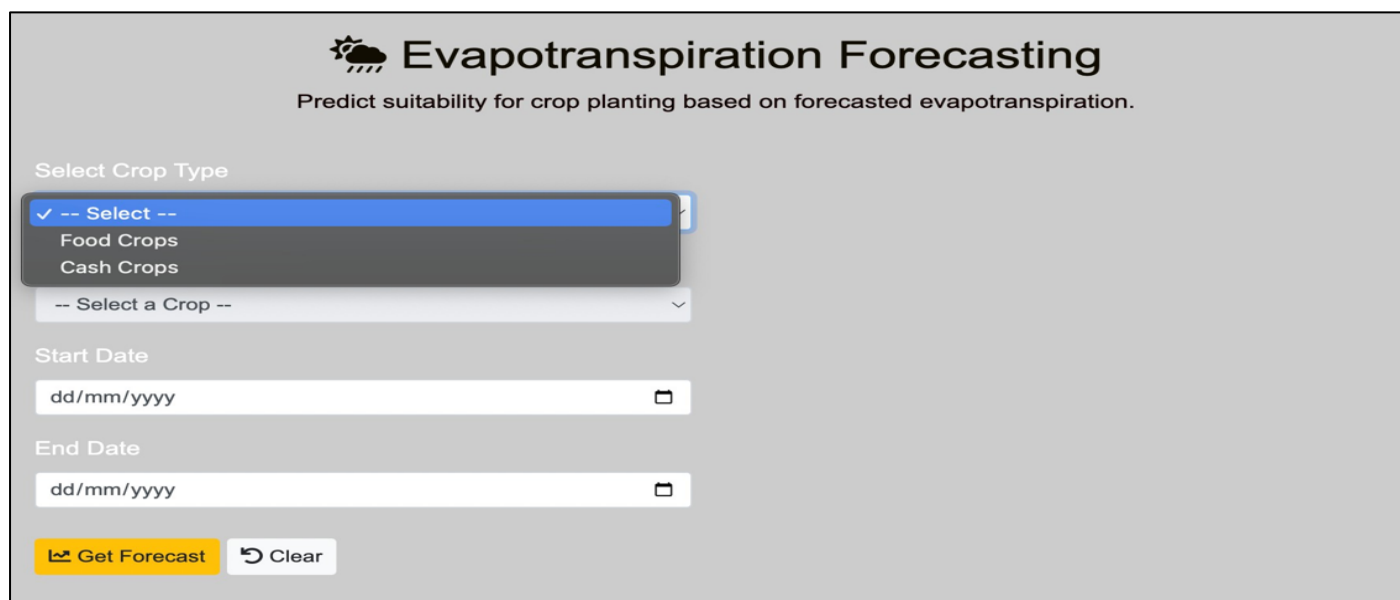
- Cocoa: 4.0-6.0 mm/day
- Coffee: 4.5-6.5 mm/day
- Rubber: 5.0-7.0 mm/day
- Oil Palm: 5.5-7.5 mm/day
- Sugarcane: 6.0-8.0 mm/day
- Tobacco: 5.0-7.0 mm/day
- Cotton: 5.5-7.5 mm/day

Figure 14 (a) - Figure (14f) shows the display of the interface.



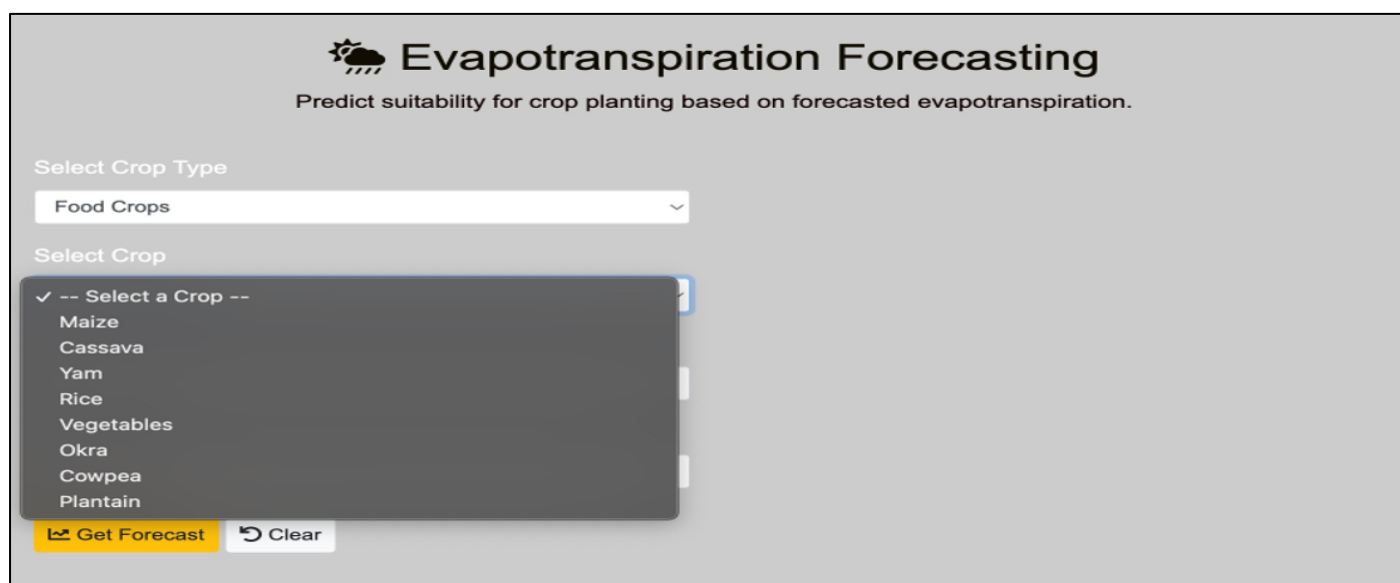
The interface features a header with a sun and cloud icon, the title "Evapotranspiration Forecasting", and the subtitle "Predict suitability for crop planting based on forecasted evapotranspiration." Below the header, there are four input fields: "Select Crop Type" with a dropdown menu showing "-- Select --", "Select Crop" with a dropdown menu showing "-- Select a Crop --", "Start Date" with a text input field showing "dd/mm/yyyy" and a calendar icon, and "End Date" with a text input field showing "dd/mm/yyyy" and a calendar icon. At the bottom, there are two buttons: "Get Forecast" (yellow) and "Clear" (white).

Fig 14 (A) Interface



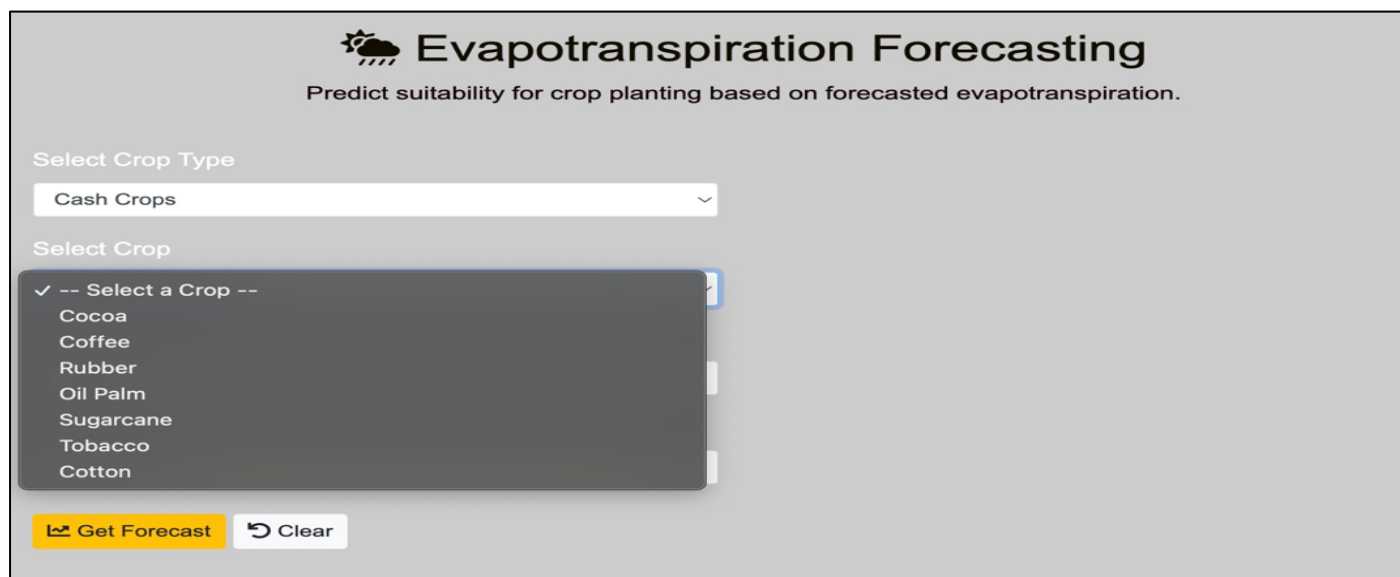
This view shows the "Select Crop Type" dropdown menu open, displaying three options: "-- Select --" (checked), "Food Crops", and "Cash Crops". The other input fields and buttons remain the same as in Fig 14 (A).

Fig 14 (B) Crop Type Dropdown



This view shows the "Select Crop" dropdown menu open, displaying a list of crops: "-- Select a Crop --" (checked), "Maize", "Cassava", "Yam", "Rice", "Vegetables", "Okra", "Cowpea", and "Plantain". The "Select Crop Type" dropdown is now set to "Food Crops". The other input fields and buttons remain the same as in Fig 14 (A).

Fig 14 (C) Dropdown for food crops



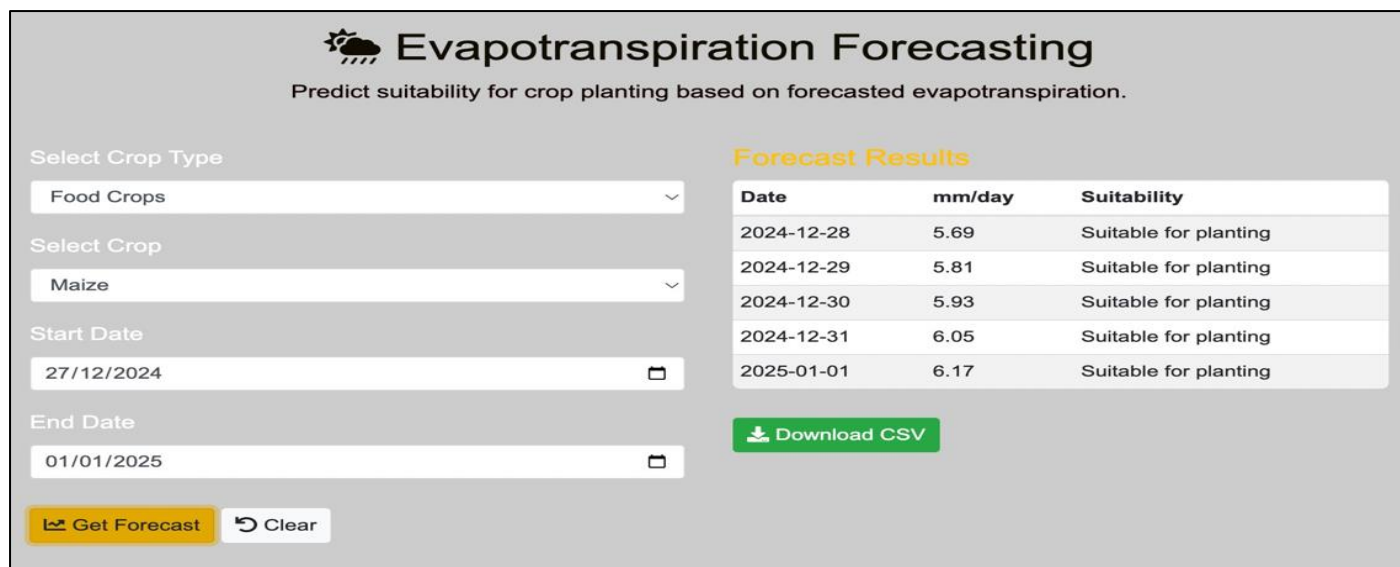
Evapotranspiration Forecasting
Predict suitability for crop planting based on forecasted evapotranspiration.

Select Crop Type
Cash Crops

Select Crop
 ✓ -- Select a Crop --
 Cocoa
 Coffee
 Rubber
 Oil Palm
 Sugarcane
 Tobacco
 Cotton

Get Forecast Clear

Fig 14 (D) Dropdown for cash crops



Evapotranspiration Forecasting
Predict suitability for crop planting based on forecasted evapotranspiration.

Select Crop Type
Food Crops

Select Crop
Maize

Start Date
27/12/2024

End Date
01/01/2025

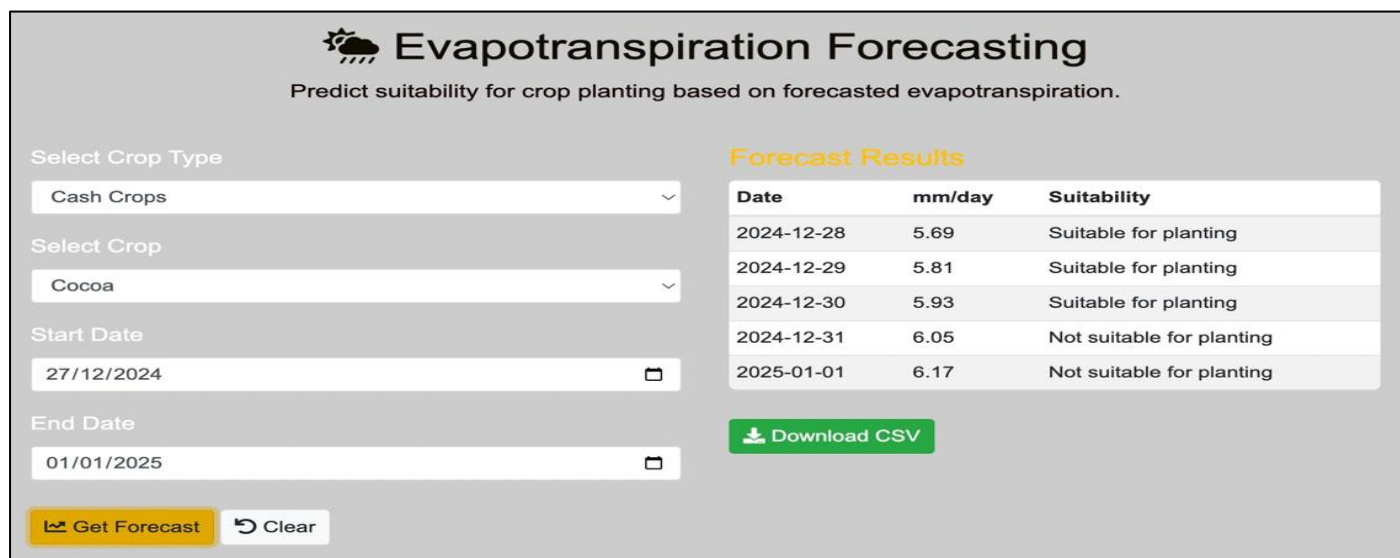
Get Forecast Clear

Forecast Results

Date	mm/day	Suitability
2024-12-28	5.69	Suitable for planting
2024-12-29	5.81	Suitable for planting
2024-12-30	5.93	Suitable for planting
2024-12-31	6.05	Suitable for planting
2025-01-01	6.17	Suitable for planting

Download CSV

Fig 14 (E) Forecast for food crops



Evapotranspiration Forecasting
Predict suitability for crop planting based on forecasted evapotranspiration.

Select Crop Type
Cash Crops

Select Crop
Cocoa

Start Date
27/12/2024

End Date
01/01/2025

Get Forecast Clear

Forecast Results

Date	mm/day	Suitability
2024-12-28	5.69	Suitable for planting
2024-12-29	5.81	Suitable for planting
2024-12-30	5.93	Suitable for planting
2024-12-31	6.05	Not suitable for planting
2025-01-01	6.17	Not suitable for planting

Download CSV

Fig 14 (F) Forecast for cash crops

VII. CONCLUSION

This study emphasize the critical role of accurate evapotranspiration (ET) forecasting in optimizing water resource management and irrigation planning for sustainable agriculture in Ogwashi-Uku, Southern Nigeria. By leveraging Long Short-Term Memory (LSTM) networks, a deep learning-based approach was developed to address objective stated in the studied.

The model was trained and evaluated using historical evapotranspiration data from Ogwashi-Uku, Southern Nigeria, covering both daily (2023) and monthly (2003–2024) ET forecasts. The results demonstrate that LSTM-based forecasting significantly improves ET prediction accuracy, achieving a Mean Squared Error (MSE) of 0.0034, Root Mean Squared Error (RMSE) of 0.0583, and Mean Absolute Error (MAE) of 0.0433 for daily ET forecasts, and MSE of 0.0005, RMSE of 0.0222, and MAE of 0.0182 for monthly forecasts. These metrics highlight the model's ability to provide reliable mid-and-long-term ET projections, essential for efficient irrigation scheduling, drought mitigation, and climate resilience strategies. Conclusively, this study contributes to the advancement of data-driven agricultural decision-making, offering a scalable and efficient tool for policymakers, farmers, and water resource managers to optimize irrigation strategies and ensure sustainable food production in Nigeria.

➤ Declaration of competing interest

The authors declare that they have no competing interests.

➤ Funding

This paper was prepared based on the research funded by Tertiary Education Trust Fund (TETFund), Nigeria through the institution Based Research (IBR) Interventions.

ACKNOWLEDGEMENT

The authors acknowledge Tertiary Education Trust Fund (TETFund), Nigeria for financially supporting this research through the institution Based Research (IBR) Interventions.

REFERENCES

- [1]. Burnash, R.J, (2020). *The NWS River forecast system catchment modeling*. In: Singh, V.P. (Ed.), *Computer Models of Watershed Hydrology*. Water Resources Publications, Highlands Ranch, CO, pp. 311e366.
- [2]. Chen, P., Heng, F. , Yuannong, L., Xiaobo, G., Yadan, D., Hongxiang, H., (2021). *Application of CAD for evapotranspiration simulation in urban areas using building information modeling (BIM)*. *Journal of Urban Planning and Development*, 147(2), 04021031.
- [3]. Egba. A. F. & Okonkwo, O. R (2020). *Artificial Neural Networks for Medical Diagnosis: A review of Recent Trends*. *Internal Journal of Computer science and Engineering Survey*, 3(11), 1-11
- [4]. Joshua C, B. Fisher, Terry A., DeBiase, Ye Qi, Ming Xu, & Allen H, (2015). *Evapotranspiration models compared on a Sierra Nevada forest ecosystem* *Environmental Modeling & Software* 783-796
- [5]. Kumar, P., Herndon, E., and Richter D. (2020). *Application of CAD for evapotranspiration simulation in irrigated agriculture using IoT sensors*. *Journal of Irrigation and Drainage Engineering*, 148(10), 04022055.
- [6]. Liu, W., T. Ye, J. Jägermeyr, C. Müller, S. Chen, X. Liu, and P. Shi, (2021). *Evapotranspiration estimation using CAD and deep learning algorithms*. *Journal of Applied Remote Sensing*, 15(2), 026501.
- [7]. Liu, D., Archer, N., Konsta, D., Garry, H., Russell K., (2016). *Evapotranspiration estimation using CAD and remote sensing*. *Journal of Applied Remote Sensing*, 10(2), 026501.
- [8]. Mehryar, M., Afshin, R., & Ameet, T. (2012). *Foundations of machine learning* (2nded.). The MIT Press Cambridge, Massachusetts London, England, ISBN 978-0-262-01825-8.
- [9]. Nwankwo, W., Ukaoha, K., Osika, A. N., Nwankwo, C. P., Oghorodi, D., Adigwe, W., Ojei, E., Irikefe, F. E.
- [10]. & Ovili, H. P. (2023). *Management of Misinformation in Critical Healthcare using Machine Learning Models*. *The IUP Journal of Knowledge Management*, 21(4), 24-47
- [11]. Olayinka A. S., Adetunji C. O., Nwankwo W., Olugbemi O. T. & Olayinka T. C. (2022). *A Study on the Application of Bayesian Learning and Decision Trees IoT-Enabled System in Postharvest Storage*. In: Pal S., De D., Buyya R. (eds) *Artificial Intelligence-based Internet of Things Systems*. *Internet of Things*. Springer, Cham. https://doi.org/10.1007/978-3-030-87059-1_18
- [12]. Shalev-Shwartz, S., & Ben-David, S. (2014). *Understanding machine learning: From theory to algorithms* (1sted.). Cambridge, USA, ISBN 978-1-107-05713-5.
- [13]. Sepp, H. (2013). *Theoretical bioinformatics and machine learning* (2nd Ed.). Wellington, New Zealand.
- [14]. Singh, R. K. , Singh, N. L. , Chauhan, R. D. , Mayur Mehta, Suryanarayana, S. V. , (2022).
- [15]. *Evapotranspiration modeling using CAD and machine learning algorithms*. *Journal of Hydrology*, 612, 128-135.
- [16]. Sharma, S, Sharma S. & Athaiya A. (2020). *Activation Functions in Neural Networks*. *International Journal of Engineering Applied Sciences and Technology*, 12(4), 310-316
- [17]. Sakshi K., Surbhi M. & Rahul R. (2014). *Basics of Artificial Neural Networks*. <https://www.analyticsvidhya.com/blog/2021/07/understanding-the-basics-of-artificial-neural-network/>

- [18]. Usman, O.L. & Adenubi, A.O. (2013). *Artificial Neural Network (ANN) Model for Predicting Students' Academic Performance*. Journal of Science and Information Technology. 2(1):23-37
- [19]. Zhang, Z. X., Sng, L. H., Yong, Y., Lin, L. M., Cheng, T. W., Seong, N. H., and Yong, F. K., (2020). *CAD- based evapotranspiration modeling for water resources management using remote sensing data*. Journal of Water Resources Planning and Management, 148(10), 04022065.